Into the Dark Serum Proteome: Personalized Features of IgG1 and IgA1 Repertoires in Severe COVID-19 Patients

Authors

Albert Bondt, Max Hoek, Kelly Dingess, Sem Tamara, Bastiaan de Graaf, Weiwei Peng, Maurits A. den Boer, Mirjam Damen, Ceri Zwart, Arjan Barendregt, Danique M. H. van Rijswijck, Douwe Schulte, Marloes Grobben, Khadija Tejjani, Jacqueline van Rijswijk, Franziska Völlmy, Joost Snijder, Francesca Fortini, Alberto Papi, Carlo Alberto Volta, Gianluca Campo, Marco Contoli, Marit J. van Gils, Savino Spadaro, Paola Rizzo, and Albert J. R. Heck

Correspondence

a.j.r.heck@uu.nl

In Brief

In serum proteome analyses, the abundant immunoglobulins are often disregarded, likely due to their intrinsic diversity. In contrast, here we portray an unconventional serum proteomics method that distinctively focuses on the "immunoglobulome'. Using affinity enrichment and proteases that selectively cleave the Fab-arms of IgG1 or IgA1, we perform clonal repertoire analysis by LC-MS, measuring qualitatively and quantitatively the most abundant immunoglobulins in a small patient cohort of severe COVID-19 patients. We highlight how this approach reveals intricate personalized health data.

Graphical Abstract

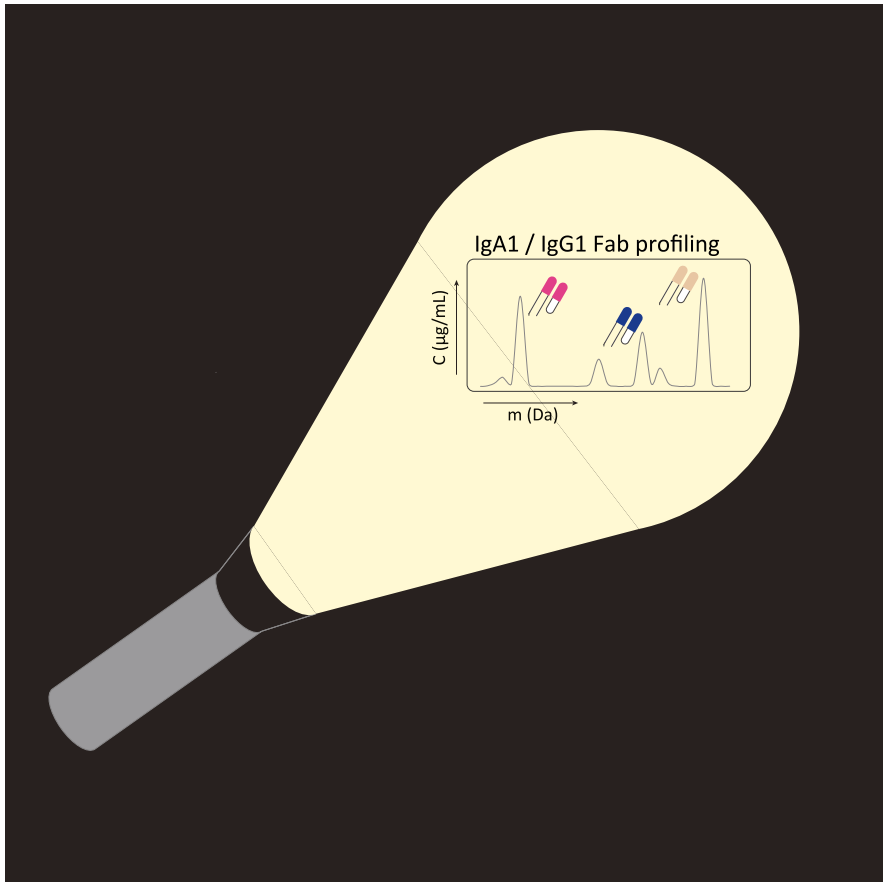

2024, Mol Cell Proteomics *23*(*1*), 100690

https://doi.org/10.1016/j.mcpro.2023.100690

Highlights

- Alternative serum proteomics approach focusing on the immunoglobulome.
- Quantitative analysis of IgG1 and IgA1 clonal repertoires of individual patients.
- Small cohort of severe COVID-19 patients is monitored longitudinally.
- Ig repertoires are highly personalized and respond markedly upon SARS-CoV2 infection.
- Ig repertoires are affected by clinical treatments.

Into the Dark Serum Proteome: Personalized Features of IgG1 and IgA1 Repertoires in Severe COVID-19 Patients

Albert Bondt[1,2,‡], Max Hoek[1,2,‡], Kelly Dingess[1,2], Sem Tamara[1,2], Bastiaan de Graaf[1,2], Weiwei Peng[1,2], Maurits A. den Boer[1,2], Mirjam Damen[1,2], Ceri Zwart[1,2], Arjan Barendregt[1,2], Danique M. H. van Rijswijck[1,2], Douwe Schulte[1,2], Marloes Grobben[3], Khadija Tejjani[3], Jacqueline van Rijswijk[3], Franziska Völlmy[1,2], Joost Snijder[1,2], Francesca Fortini[4], Alberto Papi[5,6], Carlo Alberto Volta[7,8], Gianluca Campo[9], Marco Contoli[5,6], Marit J. van Gils[3], Savino Spadaro[7,8], Paola Rizzo[4,10], and Albert J. R. Heck[1,2,*]

Serum proteomics has matured and is now able to monitor hundreds of proteins quantitatively in large cohorts of patients. However, the fine characteristics of some of the most dominant proteins in serum, the immunoglobulins, are in these studies often ignored, due to their vast, and highly personalized, diversity in sequences. Here, we focus exclusively on these personalized features in the serum proteome and distinctively chose to study individual samples from a low diversity population: elderly donors infected by severe acute respiratory syndrome corona virus 2 (SARS-CoV-2). By using mass spectrometry-based methods, immunoglobulin IgG1 and IgA1 clonal repertoires were monitored quantitatively and longitudinally in more than 50 individual serum samples obtained from 17 Corona virus disease 2019 patients admitted to intensive care units. These clonal profiles were used to examine how each patient reacted to a severe SARS-CoV-2 infection. All 17 donors revealed unique polyclonal repertoires and substantial changes over time, with several new clones appearing following the infection, in a few cases leading to a few, very high, abundant clones dominating their repertoire. Several of these clones were *de novo* sequenced through combinations of top-down, middle-down, and bottom-up proteomics approaches. This revealed sequence features in line with sequences deposited in the SARS-CoV-specific antibody database. In other patients, the serological Ig profiles revealed the treatment with tocilizumab, that subsequently dominated their serological IgG1 repertoire. Tocilizumab clearance could be monitored, and a half-life of approximately 6 days was established. Overall, our longitudinal monitoring of IgG1 and IgA1 repertoires of individual donors reveals that antibody responses are highly personalized traits of each patient, affected by the disease and the chosen clinical treatment. The impact of these observations argues for a more personalized and longitudinal approach in patients' diagnostics, both in serum proteomics as well as in monitoring immune responses.

More than 30% of the proteins in our blood are immunoglobulins. Of these, IgG1 molecules account for 20 to 30% and IgA1 for 5 to 10%. Immunoglobulins, also known as antibodies, are glycoprotein molecules produced by plasma cells, and they act as a key part of the adaptive immune response by specifically recognizing and binding to antigens derived from bacteria or viruses, thereby initiating and/or aiding in their destruction. Each human can produce a vast variety of distinct antibody-producing B cell clones, with estimates ranging from 10^{13} to 10^{18} (1, 2). This repertoire allows

From the [1]Biomolecular Mass Spectrometry and Proteomics, Bijvoet Center for Biomolecular Research and Utrecht Institute for Pharmaceutical Sciences, University of Utrecht, Utrecht, The Netherlands; [2]Netherlands Proteomics Center, Utrecht, The Netherlands; [3]Department of Medical Microbiology and Infection Prevention, Amsterdam Institute for Infection and Immunity, Amsterdam UMC, University of Amsterdam, Amsterdam, The Netherlands; [4]Maria Cecilia Hospital, GVM Care & Research, Cotignola, Italy; [5]Respiratory Section, Department of Translational Medicine, University of Ferrara, Ferrara, Italy; [6]Respiratory Disease Unit, Azienda Ospedaliero-Universitaria di Ferrara, Ferrara, Italy; [7]Department of Translational Medicine, University of Ferrara, Ferrara, Italy; [8]Intensive Care Unit, Azienda Ospedaliero-Universitaria di Ferrara, Ferrara, Italy; [9]Cardiology Unit, Azienda Ospedaliero-Universitaria di Ferrara, and [10]Department of Translational Medicine and Laboratory for Technology of Advanced Therapies (LTTA), University of Ferrara, Ferrara, Italy

‡These authors contributed equally to this work and share first authorship.

*For correspondence: Albert J.R. Heck, a.j.r.heck@uu.nl.

https://doi.org/10.1016/j.mcpro.2023.100690

humans to adequately respond to attacks by the huge variety of pathogens and other foreign elements we daily encounter. However, as shown previously by others and us, at a given moment in time, there are likely only thousands of different antibodies circulating in detectable amounts in our blood, and typically the top 50 most abundant Ig clones account for up to >90% of the complete Ig repertoire (3–6). Although belonging to the most abundant and most important proteins in serum, immunoglobulins are often depleted, in large-scale serum proteomics studies, or ignored in the data analysis, likely due to their personalized features (7–10).

Recently, we developed methods to exclusively shine our light on this "dark" serum proteome, whereby we directly affinity-purify all IgG molecules from serum or plasma and subsequently cleave of the IgG1-Fab fragments (that harbor the important antigen recognizing complementarity determining region [CDR] regions), subjecting them to mass analysis by intact Fab profiling LC-MS. Each LC-MS trace contained a few hundred unique signals (based on mass and retention time [RT]) that we considered unique clones. By spiking in recombinant IgG1 mAb standards, we were able to monitor the serum concentration of each clone in the repertoire over time (3). Next, we adapted the Fab profiling LC-MS sample preparation to target specifically IgA1, using a different affinity-capture resin, another protease to produce the Fab fragments, and recombinant IgA1 mAb standards (4). By monitoring these IgG1 and IgA1 repertoires, we observed that human plasma IgG1 and IgA1 repertoires are relatively simple (dominated by just a few hundred different clones) but also unique and highly personalized as we rarely observed the same clones in more than one donor. Moreover, in healthy donors, we found that the IgG1 and IgA1 repertoires were very stable over time. In contrast, in patients experiencing a septic episode, we noticed substantial changes in the IgG1 repertoires (3). The degree of change, however, was again highly personalized. In that case, we hypothesized that this might be due to the variety of pathogens causing illness.

Therefore, in the present study, we set out to follow up on these earlier findings by focusing on a real-life small cohort of patients, all infected with the same pathogen, namely severe acute respiratory syndrome corona virus 2 (SARS-CoV-2). This cohort consists of a subgroup of 17 patients from the ATTAC-Co study (registered at www.clinicaltrials.gov, number NCT04343053). Earlier, we sampled the serum proteomes of these patients, which allowed us to define a serum proteome signature that could be used to predict mortality in severe Corona virus disease 2019 (COVID-19) patients (9). This serum proteome signature was confirmed by similar studies appearing at the same time (10, 11).

The cohort was not designed for this study but does reflect a real-life situation in a clinic at the onset of a pandemic. By applying our methods to monitor—longitudinally and in parallel —the IgG1 and IgA1 repertoires of these patients, we aimed to address the question of how antibody repertoires react during changes in physiology of these patients. As these patients all suffered from an infection by the early variant of SARS-CoV-2, we hypothesized to observe the rise and presence of SARS-CoV-2 targeting antibodies in their serum. However, we were equally interested to see whether the unique individual clinical treatment each patient received influenced their serological Ig repertoires over time.

EXPERIMENTAL PROCEDURES

Ferrara Patient Cohort Serum Sample Collection and Chemicals

The present analysis included patients from the "Pro-thrombotic status in patients with SARS-CoV-2 infection" (ATTAC-Co) study (12–15). The ATTAC-Co study is an investigator-initiated, prospective, single-center study recruiting consecutive patients admitted to the intensive care unit (ICU) at the University Hospital of Ferrara, Italy, because of COVID-associated acute respiratory distress syndrome between April and May 2020. Inclusion criteria were (i) age >18 years; (ii) confirmed SARS-CoV-2 infection; (iii) hospitalization for respiratory failure; and (iv) need for invasive or noninvasive mechanical ventilation or only oxygen support. Exclusion criteria were prior administration of P2Y12 inhibitor (clopidogrel, ticlopidine, prasugrel, and ticagrelor) or anticoagulant drugs (warfarin or novel oral anticoagulants) known disorder of coagulation or platelet function and/or chronic inflammatory disease. SARS-CoV-2 infection was confirmed by RT-PCR assay (Liaison MDX; Diasorin) from nasopharyngeal swab specimen. Respiratory failure was defined as a PaO2/FiO2 ratio ≤200 mmHg. Clinical management was in accordance with current guidelines and specific recommendations for COVID-19 pandemic by Health Authorities and Scientific Societies. The serum and plasma samples were stored at −80 °C. The ATTAC-Co study population consists of 54 moderate-to-severe COVID-19 patients (12–15). The protocol was approved by the corresponding Ethics Committee (Comitato Etico di Area Vasta Emilia Centro, Bologna, Italy) abiding to the Declaration of Helsinki principles. All patients gave their written informed consent. In case of unconsciousness, the informed consent was signed by the next of kin or legal authorized representative. The study is registered at www.clinicaltrials.gov with the identifier NCT04343053. At the early onset of the pandemic, *i.e.*, when these patients were hospitalized, it was still very much unclear what would be the best treatments for COVID-19 patients, and therefore, it may come as no surprise that patients were not treated all in the same manner, *e.g.*, they encountered variable numbers of plasma, red blood cell, or platelet transfusions and various forms of treatment with immune-suppressing medication (Fig. 1).

In addition, longitudinal EDTA plasma samples from two healthy Caucasian donors were purchased from Precision Med. The samples were part of the 'Normal Control Collections', protocol number 7005-8200.

Experimental Design and Statistical Rationale

The subgroup of interest for the present analysis is selected starting from the 16 cases who died and was then narrowed down to five patients for which IgG and IgA data were available for all three time points. From the remaining 38 survivors, we identified 17 cases who best matched in terms of age, clinical history, and clinical presentation. Of these 17 cases, we used data for 12 with all three time points available. From the selected 12 survivors and five nonsurvivors (Supplemental Table S1), serum samples were collected at three time points: just after admission to the ICU (T1), after 7 ± 3 days (T2), and after 14 ± 4 days (T3) (Fig. 1).

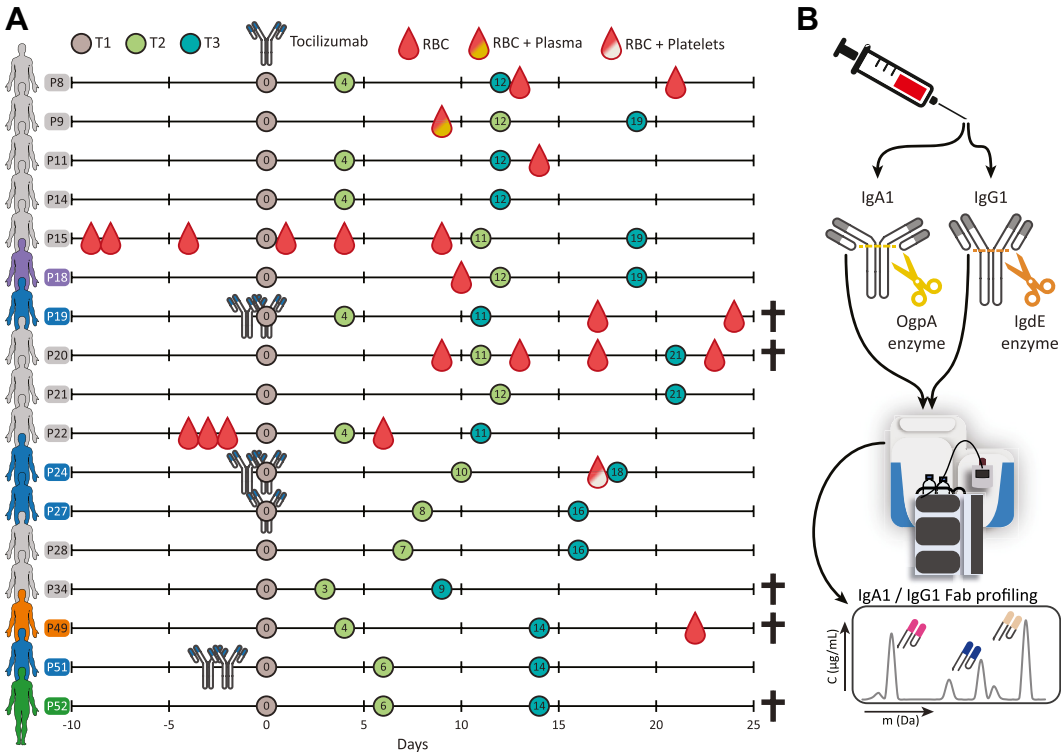

FIG. 1. **Schematic overview of the cohort, the blood sampling, and the applied method for repertoire profiling.** *A*, timeline of blood sampling with annotated relevant treatments, namely monoclonal antibody therapy (tocilizumab), red blood cell transfusion (RBC), red blood cell and plasma transfusions (RBC + Plasma), and red blood cell and platelet transfusions (RBC + Platelets). For each patient (annotated as Pxx), the first blood sample was marked as day 0 (*brown circle*; T1). The consecutive sampling time points T2 (*green circle*) and T3 (*blue circle*) are annotated with the number of days after T1. Several patients are highlighted in color, these individuals are discussed in more detail: *blue* when receiving tocilizumab monoclonal antibody therapy, *orange* when the repertoires were analyzed more in depth, and one donor in *green* for which we measured a completely aberrant serum profile at T3. Patients that did not survive are annotated with a cross. *B*, schematic overview of the IgG1 and IgA1 profiling methodology. IgA1 and IgG1 are captured from individual's blood serum and digested in the hinge region by specific enzymes OgpA and IgdE. The released Fab fragments are then separated and analyzed by intact LC-MS, resulting in either an IgA1 or IgG1 clonal profile.

Having 17 donors affected by COVID-19 and sampling blood over three time points while being hospitalized, we were able to record 102 Ig profiles, 51 for IgG1 and 51 for IgA1. As analytical controls, we added two (nonrelated) healthy donors of which we also had samples at three time-points (at 1-month intervals), extending our analysis to in total 108 Ig profiles.

IgA Sample Preparation

IgA Fab samples were prepared as described before (4). Briefly, IgAs were affinity captured using CaptureSelect IgA affinity matrix (Thermo Scientific) from 20 µl patient serum spiked-in with 200 ng of 7D8-IgA1 monoclonal antibody. After 1 h shaking incubation, the unbound fraction of the samples was collected in a fresh tube and stored at 4 °C to be used later for IgG capturing. The bound IgAs were washed, and a sialidase cocktail (SialEXO) and OgpA enzyme (OpeRATOR) were added for overnight digestion of the captured IgA. On the next day, the flowthrough from the digestion containing IgA Fabs was collected after removal of the His-tagged enzymes by Ni-NTA affinity capturing.

IgG Sample Preparation

IgG Fab samples were prepared as described before, with minor modifications (3). Briefly, IgGs were affinity captured from 85 µl of IgA affinity capturing flowthrough, substituted with 100 µl PBS and 1 µl PBS containing 200 ng trastuzumab and 200 ng alemtuzumab monoclonal IgG antibodies. The monoclonal antibodies were included for RT and mass reference and for quantification of all other detected clones. After 1 h shaking incubation, the bound IgGs were washed, and IgdE enzyme (FabALACTICA) was added for overnight digestion of the captured IgG. On the next day, the flowthrough from the digestion containing IgG Fabs was collected after removal of the His-tagged enzyme by Ni-NTA affinity capturing.

Fab LC-MS(/MS)

Fab LC-MS was performed as described before (3), with minor modifications. Briefly, Fabs were separated by reversed-phase liquid chromatography on a Vanquish Flex UHPLC instrument with a 1 mm × 150 mm MAbPac RP analytical column. The LC was coupled to an Orbitrap Lumos Tribrid (Thermo Scientific). Separate Fab chains were analyzed with a resolution setting of 120,000 (@ m/z 200) in MS1. MS/MS scans were acquired with a resolution of 120,000. MS1 scans were acquired in a range of *m/z* 500 to 4000 and MS2 scans in the range of *m/z* 350 to 5000.

Clonal Profiling Data Analysis

Data analysis of the clonal profile was performed as described before (3), with the exception of a few different settings in the BioPharma Finder deconvolution. Deconvolution was performed using

the ReSpect algorithm between 5 and 57 min using 0.1 min sliding window with 25% offset and a merge tolerance of 30 ppm. Detection of the spiked-in mAbs was set as a requirement for runs to be included. All masses with a score above 40, with an observed mass between 45,000 Da and 53,000 Da and originating from a charge state envelope with the dominant charge state above *m/z* 1000, were considered individual clones. Using the data of spiked-in mAbs (trastuzumab and alemtuzumab for IgG1 and 7D8 for IgA1), mass and RT corrections were applied. Clones were matched between runs using mass tolerance of 1.5 Da and RT tolerance of 1.0 min.

Luminex Immunoassays

SARS-CoV-2-specific Luminex Immunoassays were performed as described before (16). Briefly, Spike-trimer, the RBD (receptor-binding domain), and the nucleocapsid protein of SARS-CoV-2 were covalently coupled to Luminex Magplex beads (Luminex) at a ratio of 75 μg protein per 12,5 million beads for Spike-trimer, equimolar quantity for Nucleocapsid protein, and 3× equimolar quantity for the RBD. Fifteen beads per μl were incubated with 1:10,000 diluted serum in blocking buffer (PBS +2% bovine serum albumin +3% fetal calf serum +0.02% Tween-20), overnight at 4 °C while shaking. Beads were washed and then stained for 2 h with either Goat-Anti-Human IgG-PE or Goat-Anti-Human IgA-PE (Southern Biotech). Finally, the beads were washed and analyzed on a Magpix (Luminex). Mean fluorescence intensity values of bead and buffer-only wells were subtracted from the resulting mean fluorescence intensity values, and the results were presented as arbitrary units.

Bottom-Up Proteomics for In-Depth Sequence Insights

In-Gel Digestion—Fabs were loaded 3 μg per lane on a 4 to 12% Bis-Tris precast gel (Bio-Rad) in nonreducing conditions and ran at 120 V in 3-Morpholinopropane-1-sulfonic acid buffer (Bio-Rad). The Fab bands were cut and reduced by 10 mM tris(2-carboxyethyl) phosphine at 37 °C, followed by alkylation in 40 mM iodoacetic acid at room temperature in the dark. The Fab bands were digested by trypsin, chymotrypsin, thermolysin, and α-lytic protease, all performed at 37 °C overnight in a 50 mM ammonium bicarbonate buffer. The peptides were extracted with two steps incubation at room temperature in 50% acetonitrile (ACN), 0.01% TFA, and 100% ACN respectively, and subsequently dried in speed-vac.

Mass Spectrometry—The digested peptides were separated by online HPLC on an Dionex UltiMate 3000 (column packed with Poroshell 120 EC C18; 50 cm × 75 μm, 2.7 μm, Agilent Technologies) coupled to an Orbitrap Fusion mass spectrometer. Samples were eluted over a 90 min gradient from 9 to 55% Buffer B (80:19.9:0.1 ACN:MQ:FA) in Buffer A (99.9:0.1 MQ:FA) at a flow rate of 0.3 μl/min. The MS resolution setting was 60,000 in MS1. MS1 scans were obtained with a standard automatic gain control target, a maximum injection time of 50 ms, and a scan range of *m/z* 350 to 2000. The precursors were selected with a 3 Th window and fragmented by stepped high-energy collision dissociation as well as electron-transfer high-energy collision dissociation. The stepped high-energy collision dissociation fragmentation included steps of 25, 35, and 50% normalized collision energies. Electron-transfer high-energy collision dissociation fragmentation was performed with calibrated charge-dependent electron-transfer dissociation parameters and 27% normalized collision energy supplemental activation. For both fragmentation types, MS2 scans were acquired at a 30,000 resolution, a 4e5 automatic gain control target, a 250 ms maximum injection time, and a scan range of *m/z* 120 to 2000.

Peptide Sequencing From MS/MS Spectra—MS/MS spectra were used to determine *de novo* peptide sequences using PEAKS Studio X (version 10.6). We used a tolerance of 20 ppm and 0.02 Da for MS1 and MS2, respectively. Enzyme specificity was set as RK for trypsin, AVST for aLP, WLMYF for chymo, nonspecific for TL. Carboxymethylation was set as fixed modification of cysteine and variable modification of peptide N termini and lysine. Oxidation of methionine and tryptophan and pyroglutamic acid modification of N-terminal glutamic acid and glutamine were set as additional variable modifications. PEAKS does not allow to set semispecific or missed cleavages. The CSV file containing all the *de novo*-sequenced peptide was exported for further analysis.

Template-Based Assembly Via *STITCH*—The CSV files exported from PEAKS were used as input dataset for STITCH (1.1.2-windows) template-based assembly (17). The human antibody database from ImMunoGeneTics was used as template. The cutoff score for the *de novo*-sequenced peptide was set as 90, and the cutoff score for the template matching was set as 10. All the peptides supporting the sequences were examined manually.

RESULTS

Using experimental approaches detailed previously, we purified either IgG or IgA from the serum of the donor and used subsequently the enzyme IgdE or OgpA to cleave off and extract the Fab fragments of all IgG1 and IgA1 clones, respectively (3, 4). These Ig Fab fragments cover all six hypervariable CDR regions of the heavy and light chain, which results in each Fab having a characteristic mass in the range of 45 to 49 kDa. Separation of all these Fab molecules and analyzing them by intact mass LC-MS provides a view at the IgG1 or IgA1 clonal repertoire. By spiking in recombinant mAbs of known quantity, the concentration of each of the detected endogenous Fabs can be obtained. In this manner, the recorded Ig profiles provide a qualitative and quantitative measure of the 50 to 500 most abundant antibodies in the serum of the donors.

Huge Variety in Total Levels of IgG1 and IgA1 in Individual Patients

Besides information on the concentration of each individual Ig clone in the repertoire, our data also provide a means to measure the total levels of IgG1 and IgA1 in the individual patients at each time point of sampling. We quantified the total levels of IgA1 and IgG1 by summing up the total concentrations of Fab molecules derived from the repertoires. The total IgG1 and IgA1 levels in each donor were found to vary widely, ranging from 0.5 to 25 mg/ml for IgG1 and 0.1 to 4.5 mg/ml for IgA1. These IgG1 and IgA1 levels do not necessarily correlate per donor as IgG1/IgA1 ratios also ranged from 0.3 to 25, with, quite remarkably, several donors exhibiting higher IgA1 levels than IgG1 (Fig. 2*A* and Supplemental Table S2). To illustrate these variations, we highlight the levels of a few selected patients in Figure 2*A*, from which these observations are apparent. By monitoring these total IgG1 and IgA1 levels in the serum of the donors, we already observed that patient's serological Ig levels are widely variable.

Several previous serum proteomics studies using mass spectrometry-based peptide-centric (bottom-up) approaches revealed a decreased survival rate in COVID-19 patients with higher IgA1 levels (9–11). In Figure 2*B*, we present a

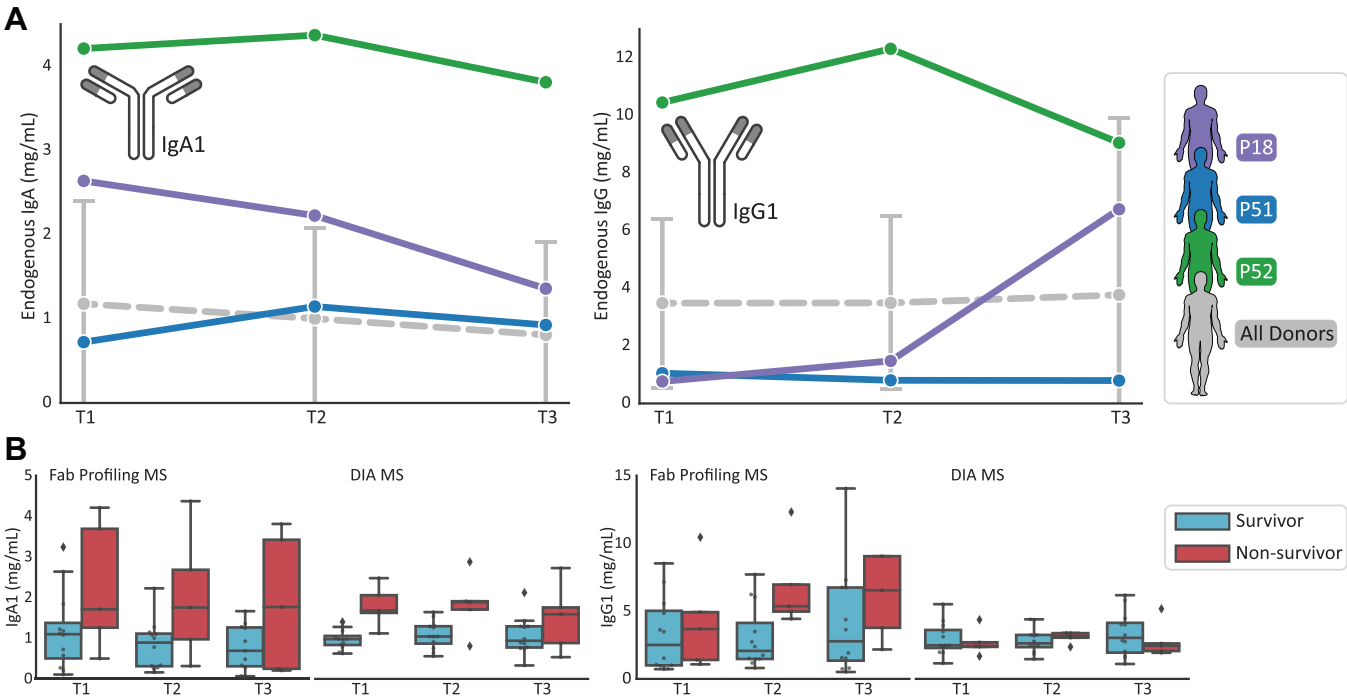

FIG. 2. **Total levels of IgG1 and IgA1 in individual patients.** *A*, for three patients (P18, P51, and P52) levels of IgA1 (*left*) and IgG1 (*right*) are depicted as determined by direct Fab profiling LC-MS (FP-MS), illustrating high variability. In *gray*, the average concentration of all donors is plotted. *B*, comparison of total levels of IgG1 and IgA1 as measured by FP-MS and by shot-gun data-independent acquisition (DIA-) MS. For quantification by FP-MS, the sum of all unique Fab concentrations was taken. For shot-gun proteomics, quantification was based on unique peptides of the constant regions of either IgG1 or IgA1. Although the data for the FP-MS approach are limited to a subcohort of the data gathered for the DIA-NN approach, the results are very much in agreement with each other, indicating that IgA1 levels in nonsurvivors are on average relatively higher than in survivors, especially at the earliest timepoints. *Diamonds* outside the box and whiskers indicate outlier values.

comparison of our quantification with the data from the study of Völlmy *et al.* (9) who measured IgA1 and IgG1 levels in a larger subset of the same cohort of 17 survivors and 16 nonsurvivors. Our current findings corroborate the earlier serum proteomics data, as we here also observe that IgA1 levels in nonsurvivors are higher at time point 1 and 2 and possibly also at time point 3. Overall, we observe a consistency between the serum proteomics data and Fab-profiling–based data on the levels of IgG1 and IgA1, which further validates both the reproducibility in protein quantification by using these two very different methods and the association of high IgA1 levels with poor COVID-19 outcome, at least in severe hospitalized patients.

IgA1 and IgG1 Clonal Profiles Are Unique for Each Donor

We next compared all the clonal profiles of IgG1 and IgA1 qualitatively and quantitatively. For each clone with a specific RT and molecular weight ($^{[RT]}[Clone\#]_{[Mw]}$), we assessed its concentration and compared it to clones having exactly the same $^{[RT]}[Clone\#]_{[Mw]}$ in all the other profiles. Interestingly, but in agreement with what we reported earlier, each unique clone was generally only detected in a single donor, albeit then mostly at all three time points of blood sampling. To provide an overview of all the data, we used a correlation score comparing each IgG1 or IgA1 profile. In Figure 3, a correlation matrix is shown comparing, on the left, all IgA1 profiles and, on the right, all IgG1 profiles, obtained for all 17 patients (and the two healthy controls) at each of the three consecutive time points.

Nevertheless, during disease development, we do observe very substantial changes in the patient-specific IgG1 or IgA1 repertoires or both. For instance, in P52, the IgA1 profiles are nearly identical at all measured time points, whereas the IgG1 profiles show quite dramatic changes over time. In contrast, in P14, the IgA1 profiles do change more over time than the IgG1 profiles. By checking the patients' medical treatment records, we found that administration of blood products, even including plasma (P9), had no significant impact on the Ig repertoires we measured. Comparing, for example, changes within P8 (no blood products between each of the sampling points) and P9 (patient who received red blood cell (RBC) + plasma between T1 and T2), there were more changes in the clonal profiles of patient P8 (Fig. 3).

Disease-Related Drastic Changes in the Serum IgG1/IgA1 Repertoires

Over time, several patients started to produce a single or a small number of very abundant IgG1 or IgA1 clones, indicated

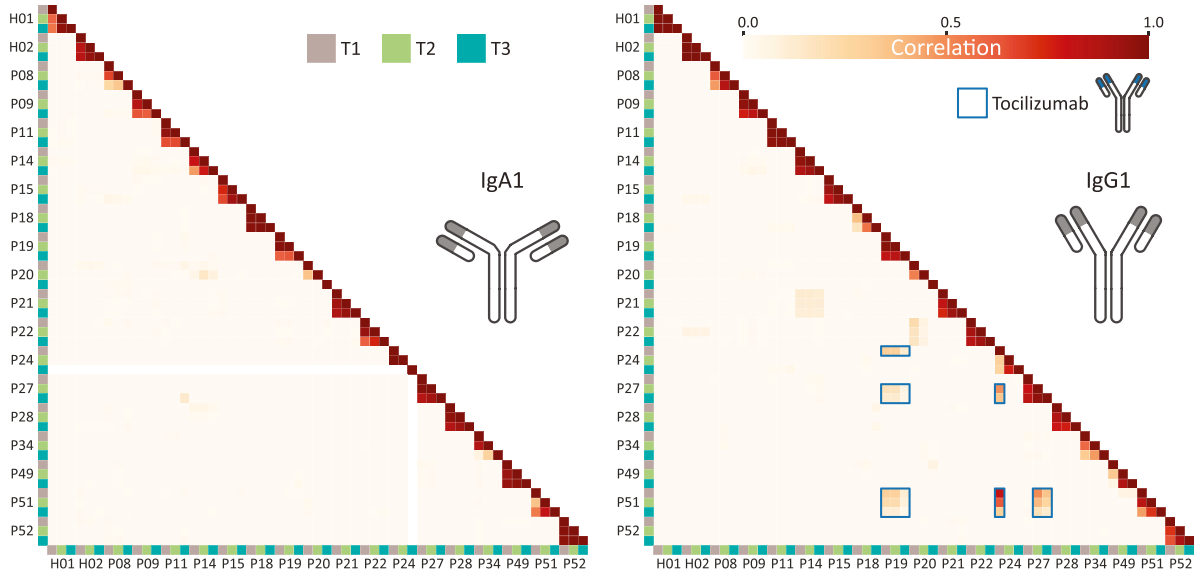

FIG. 3. **IgA1 and IgG1 clonal profiles are unique for each donor.** Correlation between patient–antibody repertoires for IgA1 (*left*) and IgG1 (*right*) for each time point as indicated by the *color-coded squares* (T1: *brown*, T2: *green* & T3: *blue*). These correlation plots are based on concentrations of all clones detected, counting the overlap in clones having identical retention time and mass in the LC-MS Fab traces. The degree of correlation is shown in a color scale from *white* to *red*, where a value of zero indicates no correlation, and a value of 1 indicates the samples are identical. The IgA1 repertoires reveal close to zero correlation between samples of different patients, but between time points within one patient generally a high correlation is observed. The IgG1 repertoires show a similar trend as IgA1, with some notable exceptions indicated by the *blue boxes*. This unexpected overlap in repertoires originates from high concentrations of a single IgG1 these patients have in common, which we show later to be tocilizumab. Disregarding the tocilizumab IgG1, the data reveal that both IgA1 and IgG1 clonal profiles are explicitly unique for each donor. P24 was included although no IgA data were obtained for T3. At the *top*, H01 and H02 show data obtained from the plasma samples originating from two healthy donors, whose blood was sampled longitudinally at 0, 1, and 2 months, here included as controls.

by high area under the curve values in clonal dominance scoring (Fig. 4*A*). We found a lot of individual variation, and no significant differences were observed between survivors and nonsurvivors. In Figure 4*B*, we showcase the profiles of a single donor, P49 (nonsurvivor). In this donor, we observed extremely high clonal dominance in IgA1 for all time points and a steep increase over time in clonal dominance for IgG1 (note the y-axis change for IgG1). Similarly, donor P52 showed a stable high clonal dominance for IgA1 and an increase over time for IgG1 (Fig. 4*A* and Supplemental Fig. S1). Of note, these extreme high concentrations of single Ig clones may be overestimation, as these numbers are outside the typical calibration regime of our method, which is in between 2 to 80 μg/ml.

Since the patients had all recently been infected with SARS-CoV-2 virus, we hypothesized that these prominent changes in the repertoires could originate from antibodies produced to bind and/or neutralize the virus, supported by previous observations that severe ICU patients have higher specific antibody titers (18). To probe whether this indeed was the case we used, a complementary Luminex bead-based binding assay measuring total IgG or IgA binding to a variety of SARS-CoV-2 virus antigens, namely the Spike-trimer, the RBD, and the nucleocapsid protein. Of note, these assays probe total IgG or IgA binding and thus do not distinguish in between IgG1/IgG2/IgG3/IgG4 or IgA1/IgA2. Not surprising, as all patients suffered from severe COVID-19, nearly all patients displayed very strong responses against these antigens (see Supplemental Table S3). For many patients, these responses were already substantial at T1, but for others, a strong response was only observed by T2 or T3. Interestingly, while for IgG responses, an increase in binding was observed from T1 to T3 in 10 of the 17 patients, and for IgA, the detected levels declined in the majority of patients, particularly for the nucleocapsid response (15/17). This observation suggests that the IgA1 response preceded the IgG response, which is in line with previous data on SARS-CoV-2 infection (19).

For the exemplary patients P49 and P52, we observed as hypothesized a 10-fold to almost 100-fold stronger response at T2 and T3 compared to T1 and more pronounced for IgG than for IgA (Fig. 4*C*).

Characterization of the Sequences of the Putative SARS-CoV-2 Targeting IgG1/IgA1s

Next, we sought to sequence *de novo* the most abundant IgG1 and IgA1 clones from the two patients P49 and P52 by using an integrative approach combining peptide-centric and protein-centric MS data. This approach enabled us to fully sequence the most abundant IgG1 and IgA1 clones as present in the sera of patient P49 and P52 (Fig. 5*A*).

In this case, by using just the protein-centric middle-down approach, we obtained confident identification of the closest-related germline sequences. This revealed that the light chains

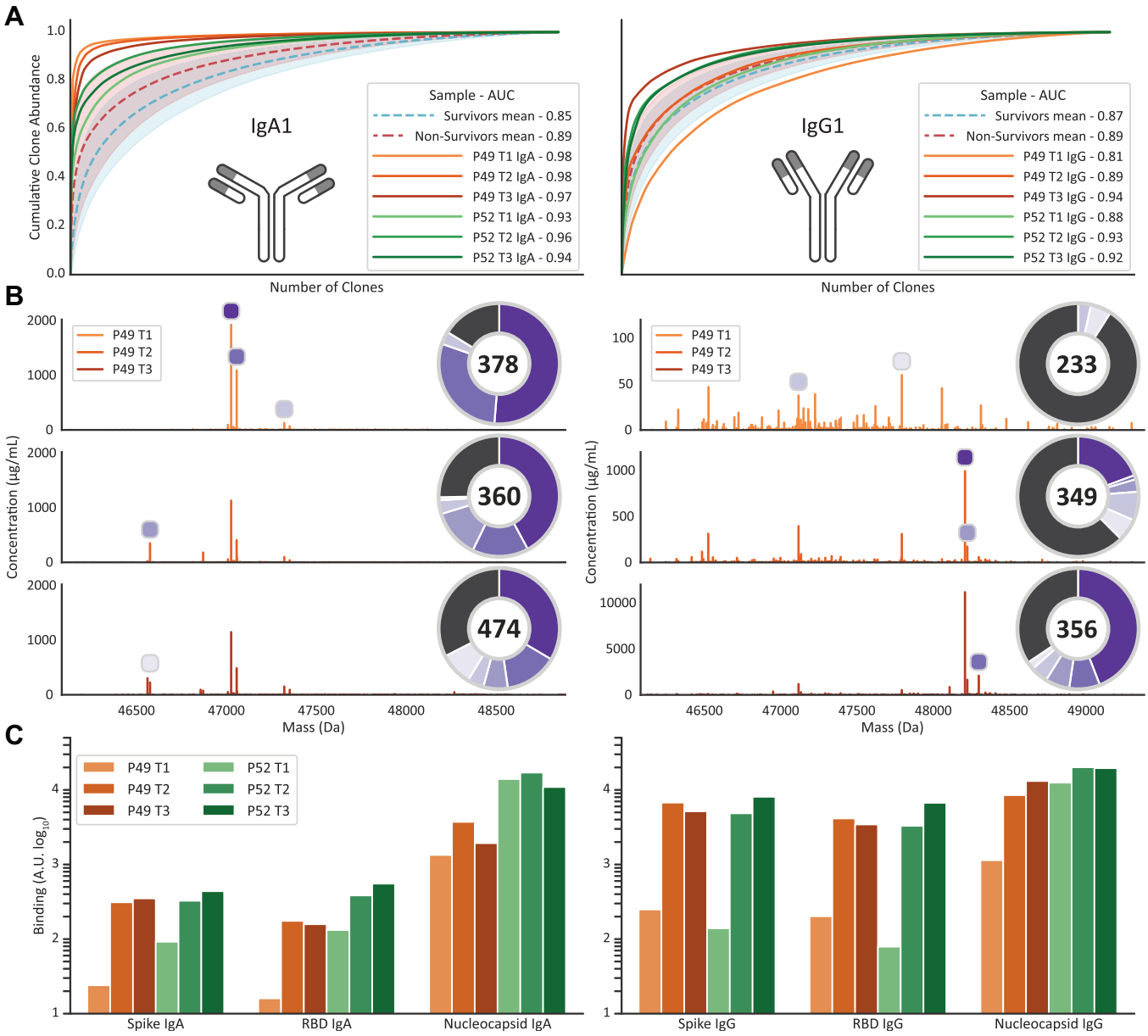

FIG. 4. **Antibody responses to SARS-CoV-2 can result in clonal profiles dominated by a small number of clones.** *A*, clonal dominance scoring plot. For each serum sample, clones are normalized and sorted by abundance. The cumulative abundance of all clones is plotted as curve, and the area under the curve (give in the legend) is a measure of how dominant/dispersed the clonal repertoire of the sample is. The panels show clone dominance scores for IgA1 (*left*) and IgG1 (*right*). The *red dashed line* shows the mean of all nonsurvivor samples, and the *green dashed line* for the survivors. The *opaque colored areas* show one standard deviation from the displayed mean. The two patients with highest clone dominance score have been highlighted, P49 in *orange* and P52 in *green*. *B*, Fab mass profiles of P49 IgA1 (*left*) and IgG1 (*right*), with relative clone abundances also provided in the pie charts. The pie chart shows the proportion of abundance for each of the top five most intense clones; the *dark gray slice* shows the proportion of the remainder of all other detected clones. The number within the pie chart shows the total number of identified clones within the serum sample. The peaks highlighted in the mass profile correspond with matching color to the slices of the pie chart. *C*, SARS-CoV-2 antigen binding monitored by a Luminex assays probing the binding of total IgA (*left*) or IgG (*right*) to the antigens; spike-trimer, receptor-binding domain (RBD), and nucleocapsid protein. SARS-CoV-2, severe acute respiratory syndrome corona virus 2.

of these clones possess limited divergence from the germline sequences. For the more diverged Fd chains, we additionally relied on the peptide-centric data to support or correct the protein-centric germline sequence prediction. Integration of the protein- and peptide-centric data allowed us to obtain accurate sequences, as corroborated by very close (within 1 Da) mass matches (Supplemental Tables S4–S8) and extensive coverages of the final sequences (Supplemental

A

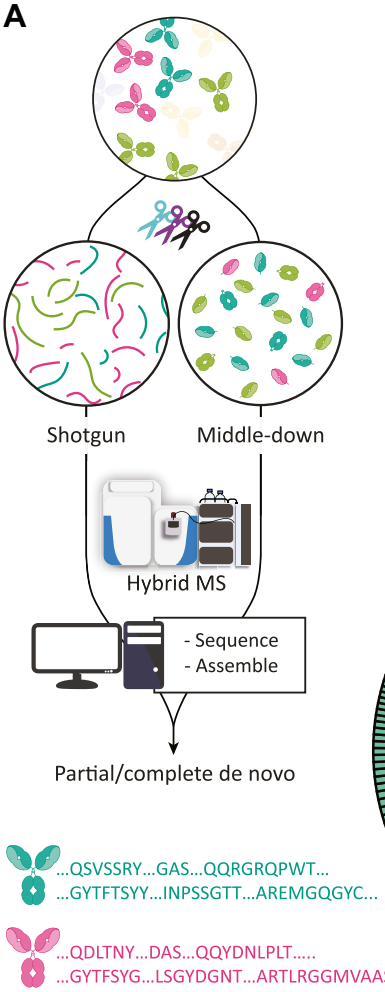

B

Donor	Ig	Chain	V-allele	J-allele	SHM [%]	CDR3 Length
P49	A1	L	IGLV3-1*01	IGLJ2*01	13	9
		H	IGHV3-9*01	IGHJ1*01	21	16
	G1	L	IGKV3-20*01	IGKJ1*01	5	9
		H	IGHV1-46*01	IGHJ4*01	5	18
P52	A1	L	IGLV1-51*01	IGLJ3*02	6	11
		H	IGHV4-61*11	IGHJ5*02	12	20
	G1	L	IGKV1-33*01	IGKJ4*01	2	9
		H	IGHV1-18*01	IGHJ4*01	7	17

C

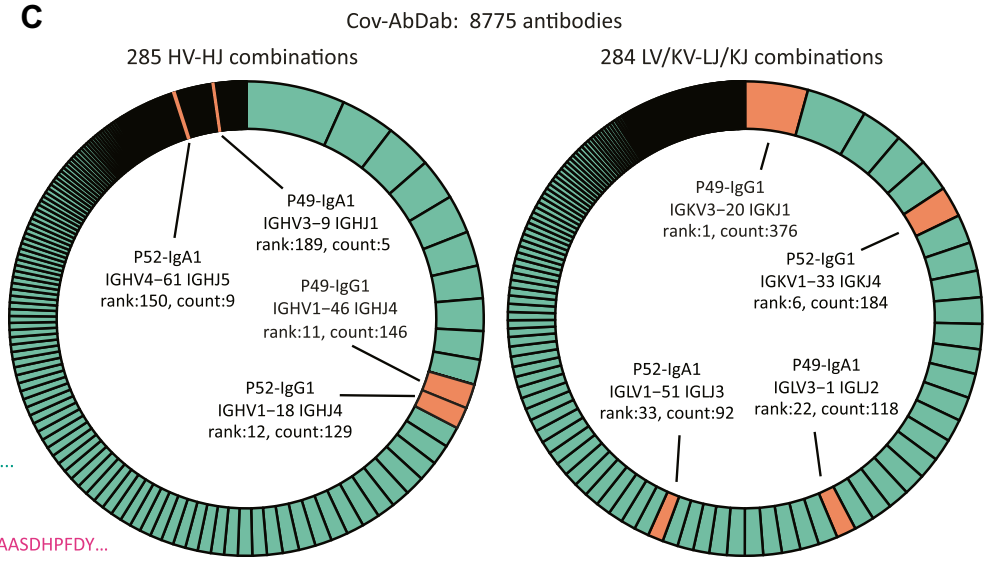

FIG. 5. ***De novo* sequencing combining peptide- and protein-centric approaches reveals that the dominant clones in P49 and P52 exhibit sequence features alike those deposited in the Cov-AbDab database of antibodies that bind and/or neutralize SARS-CoV-2.** *A*, abundant IgA1 and IgG1 clones were fully *de novo* sequenced using an integrative MS approach, combining peptide-centric (shotgun) and protein-centric (*middle-down*) approach. In the peptide-centric approach, the Fab molecules were digested in parallel with a mix of proteases to provide a set of large set overlapping peptides covering the sequence of the Fab. In the protein-centric MS approach, the Fab molecules mass-selected and fragmented with electron-transfer dissociation providing sequence tags and mass-restraints that were used to score and refine the sequences predicted from the *bottom-up* approach. The protein-centric approach was performed both at the intact Fab-level and following reduction of the disulfide bridges in the Fab, by mass-selecting ions of either the Fab light-chain or Fd heavy chains. *B*, overview of the best matching germline alleles, the amount of somatic hypermutations and the CDR3 lengths for the fully sequenced most dominant IgG1 and IgA1 clones from the serum of P49 and P52. *C*, assignment (depicted in *orange*) of the IGHV-IGHJ and IG[K/L]V-IG[K/L]J gene pairs from the here determined clones (see 5B) among the unique pairs in the database of SARS-CoV-2-related antibodies (8775 total entries in Cov-AbDab, with categories depicted in *green* in the donut charts). The antibodies in the Cov-AbDab database are primarily discovered by B cell sequencing. Especially, the germline sequences from the IgG1 clones identified in this study match well within some of the most copious categories in the Cov-AbDab database. CDR3, complementarity determining region 3; Cov-AbDab, COVID antibody database; SARS-CoV-2, severe acute respiratory syndrome corona virus 2.

Fig. S2). Compared to the germline templates, the mature sequences present in the serum of P49 and P52 showed varying degrees of somatic hypermutation, with IgG1 molecules demonstrating less variability than IgA1 molecules (Fig. 5*B*). The CDR3 lengths were as expected longer for the V-D-J gene-encoded Fd chains (16–20 residues) than for the V-J gene-encoded light chains (9–11 residues).

Next, we explored how the here derived sequences compared to the 8775 human sequences deposited in the SARS-CoV-specific database of antibodies (Cov-AbDab, version of 26th July 2022; (20)). By looking at the frequencies of unique IGxV and IGxJ combinations, we estimated the gene usages among these 8775 deposited human antibodies. Among the 285 and 284 unique entries (for light and Fd

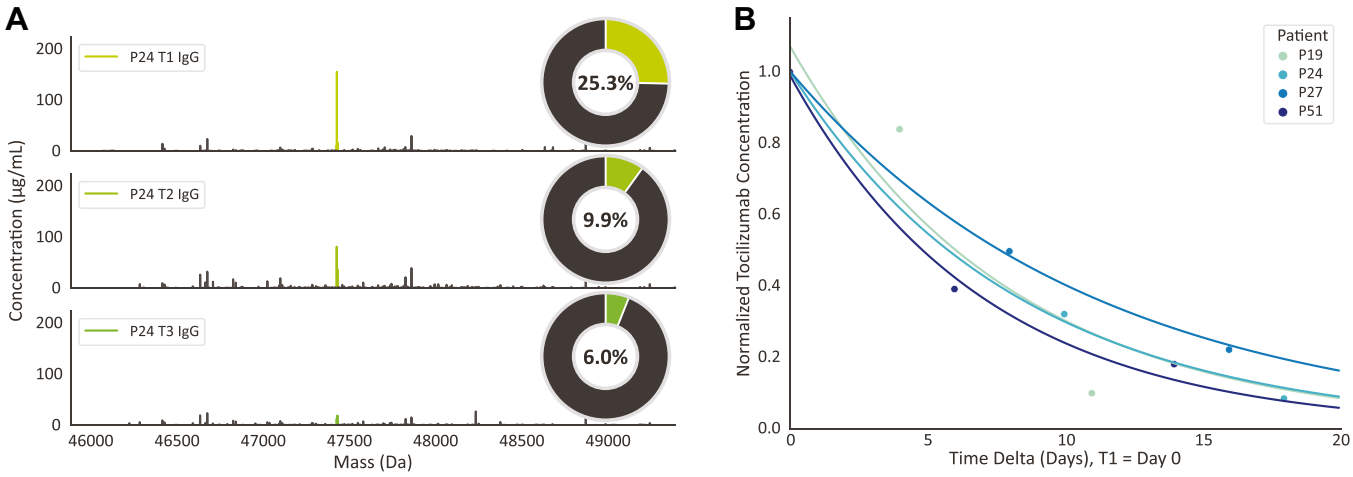

FIG. 6. **Administered tocilizumab can dominate the IgG1 serum profile but is rapidly cleared.** *A*, deconvoluted Fab mass profiles of P24 at three consecutive sampling points. Each peak represents a unique Fab (based on their unique mass and retention time), and the peak height indicates the clonal concentration. *Colored peaks* represent tocilizumab, and all other peaks are endogenous IgG1 clones. The pie chart shows the contribution of tocilizumab to the total IgG1 repertoire (based on concentrations). *B*, monitoring tocilizumab clearance and determination of its half-life in patient serum. T1 was normalized to concentration of 1 and set to day 0. Samples T2 and T3 were normalized to T1. An exponential decay curve was fitted using a nonlinear least *squares* fit. From this curve, the half-life was determined to be ~5.9 days for each of the four patients to which tocilizumab had been administered.

chains, respectively), the here obtained germline sequences for the patient IgG1 molecules scored very well, ranking as top 10 or top 20 for the Fd and light chains, respectively (Fig. 5*C*). When we searched the Cov-AbDab repository for unique light-heavy combinations that match the clones from this study, we found that the best scoring IgG1 clone from P49 again showed a high-ranked match (Supplemental Fig. S3). In contrast, the germline sequences here determined for the IgA1 molecules were less frequently present in the Cov-AbDab database.

Although we do not yet have unambiguous proof that the IgG1 and IgA1 clones sequenced here by us have binding or neutralizing activity against SARS-CoV-2 virus, the Luminex data and data from this meta-analysis against the Cov-AbDab database make them very likely candidates.

Quantitative Monitoring of Tocilizumab in the Serum IgG1 Repertoire

The data on IgG1 and IgA1 clonal repertoires revealed that individuals hardly share any Fab clones. Therefore, we were intrigued to detect a substantial overlap between the IgG1 profiles of a small subgroup of patients (namely P19, P24, P27, and P51; Fig. 3). Closer inspection revealed that this overlap could be fully attributed to a single clone, whose Fab fragment consistently had a RT of 18.6 min and an Mw of 47,441 ± 1 Da in the LC-MS data. We hypothesized that this could be due to treatment of these patients with a therapeutic monoclonal IgG1 used for the treatment of rheumatoid arthritis and systemic juvenile idiopathic arthritis and recently also for COVID-19 (21). Indeed, inspection of the clinical reports for these patients revealed that they had been treated with tocilizumab, a humanized IgG1 acting as interleukin-6 receptor antagonist. Based on its protein sequence (available on drugbank.com), we found a close match between the mass observed in the patient serum repertoires and the theoretical mass of the tocilizumab Fab (Mw = 47,442.02 Da), accounting for the glutamine to be in a pyroglutamate form. In our cohort, four patients did receive tocilizumab *via* intravenous dosing, whereby some of them received repetitive injections (Fig. 1). As tocilizumab is a humanized IgG1 antibody, in our experimental approach, it will be copurified with all endogenous IgG1 clones present in the serum. Consequently, we detected and were able to quantify the concentration of tocilizumab in parallel to the concentrations of the endogenous IgG1 clones present in the IgG1 repertoire of these patients.

The total concentrations of IgG1 and the concentration of tocilizumab in the patients P19, P24, P27, and P51 as measured in the serum are shown in Supplemental Table S9. In Figure 6*A*, mass plots depict the measured IgG1 profiles of P24, whereby the peak for tocilizumab "clone" is color coded. The pie charts shown as insets in Figure 6*A* depict the relative contribution of the tocilizumab clone to the full IgG1 repertoire, with alike data for the other patients provided in Supplemental Table S9. Strikingly, tocilizumab was often the most abundant antibody in the sera of these patients, with a concentration of 0.20 to 0.30 mg/ml after a single dose.

The FDA recommended intravenous tocilizumab dosing for treatment of COVID-19 is 8 mg/kg tocilizumab with a maximum dose of 800 mg, dependent on disease severity. The patients in our cohort received between 2.4 and 9.4 mg/kg tocilizumab. The total volume of blood in adult human beings can be estimated using the formula

70/sqrt(body mass index [BMI]/22) ml/kg (22), of which approximately 50 percent is serum. Thus, with a dose of 640 mg, the initial concentration of tocilizumab would be approximately 0.27 mg/ml in a patient with a BMI of 23 (*e.g.*, patient P19) or 0.19 mg/ml in a patient with a BMI of 38 (*e.g.*, patient P24). Among the patients and serum samples, we measured the tocilizumab concentrations were in between 0.03 and 0.55 mg/ml (Supplemental Table S9). In all these patients, we did observe a decay in abundance of tocilizumab over time, following the intravenous initial dosing. We looked at this decline (Fig. 6*B*), normalizing for each patient on the abundance at T1. Pleasingly, in all these patients, we detected a similar decline in tocilizumab abundance, from which we estimated an average half-life of tocilizumab in the serum of these older and severe COVID-19 patients of about 5.9 days. These findings agree well with data from the Centre for Evidence Based Medicine (https://www.cebm.net/covid-19/tocilizumab/) and literature (23).

Defining an Outlier Serum Sample by IgG1 and IgA1 Repertoire Profiling

IgG1 and IgA1 repertoires are very unique for each individual, not changing that much over time in healthy donors, but adapting to changes in physiology as demonstrated here for patients suffering from COVID-19. Still, even in the more changing repertoires of severely ill donors, these repertoires correlate over time much more with each other than with those of other donors. Therefore, we were somewhat puzzled by the behavior observed for P20 at T3 (Fig. 3 and more in detail Supplemental Fig. S4*A*). Both the IgG1 and IgA1 repertoires at T1 and T2 showed a good correlation with each other. In sharp contrast, the IgG1 and IgA1 repertoires measured for the sample taken at T3 contained no clones that did overlap with the repertoires measured at T1 and T2. Assessing the antibody responses of these sera to the SARS-CoV-2 antigens also revealed that the serum at T3 was a real outlier, as it did not reveal any significant response against any of the probed antigens, whereas these responses were substantial at T1 and T2 (Supplemental Fig. S4*B*). From all these data, we need to conclude that the serum annotated as T3 for patient P20 was very likely misannotated and originated from another donor, not infected with SARS-CoV-2. Although this is evidently an unwanted result, it confirms again clearly that both IgG1 and IgA1 repertoires are highly unique and personalized and may even be used to track serum samples back to individual patients. Notably, such a miss-annotated serum sample is easily picked up by the current Ig repertoire approach but harder to elucidate in more standard serum proteomics studies. With this hindsight, we did remove this time point from our earlier analysis (9) and fortuitously discovered that exclusion of this time-point did not change our major findings. As a general warning, it can be questioned whether such a mix-up of samples is exclusive for our study, or whether other even much higher high-throughput serum proteomics studies may be troubled by such "human mistakes". Fab profiling, as shown here, can help in such cases as it provides donor unique signatures.

DISCUSSION

Only recently, it has become feasible to obtain detailed insights into the circulating human antibody repertoire. We and others have shown that these repertoires are unique for every donor and that they may differ from the repertoire as observed from B cell analysis (3, 4, 24). Our previous studies involved patients with a variety of infecting agents or healthy subjects. Therefore, in the current study, we aimed to rule out that the diverse response to infection was due to the infecting entity by including patients infected by the same pathogen (here: SARS-CoV-2). Again, the donors show very different responses. We see for several donors a strong and early recognition of virus proteins by IgA, whereas a strong IgG1 response occurs somewhat more delayed (Supplemental Table S3), which is in line with previous reporting on the SARS-CoV-2 response (19). In other donors, we observed a continuously high IgG response during the analyzed time frame indicative of an early IgG1 response, and in others, the signal is fading out. The detected IgG1 and IgA1 repertoires change over time, but the amplitude of these responses and their time course seems to be a highly personalized feature. It is therefore most likely that other immunological factors, presumably donor-specific, are regulating personalized responses to a COVID-19 infection. Furthermore, not all common features of the changes in repertoire may be captured within the available time frame of this study. Intriguingly, several studies have previously shown a decreased COVID-19 survival rate in correlation with high IgA1 levels (9–11), similar as our findings presented in Figure 2*B*. On the other hand, we present in Figure 4*A* that the nonsurvivors score higher in clonal dominance; in other words, they more often have a small number of clones dominating their IgA repertoire. This suggests that potentially only a limited number of clones are present in harmful concentrations or act in the immune response in a harmful manner and not that high IgA1 by itself is causing poor survival. The highly personalized nature of the antibody repertoire and response to the pathogen would require a higher number of donors to reach statistical significance for these statements, if the personalized nature does not preclude statistics to begin with.

Through advances in mass spectrometry, it has become within reach to sequence recombinant antibodies *de novo* by mass spectrometry using either protein-centric (top-down) or peptide-centric (shotgun or bottom-up) proteomics approaches (17, 25–29) or combinations thereof. However, to do this on endogenous serum clones, in a background of many highly similar antibodies, represents still an arduous undertaking. Particularly, in bottom-up proteomics—whereby proteins are digested into smaller peptides—it remains difficult to

connect the peptide sequencing data to the antibody of origin, since large portions of antibody sequences are shared between all clones. Top-down and middle-down approaches targeting the intact Fab or LC and Fd fragments may then come to the rescue, especially as some fragmentation methods, such as electron-capture dissociation and electron-transfer dissociation, produce sequence tags covering the highly variable clone-specific CDR regions (30–32). We recently provided a proof-of-concept that by using an integrative approach combining peptide-centric and protein-centric MS data, it is possible to sequence *de novo* a full (abundant) Fab of a single clone, even in the background of serum (3). In the present study, we were able to obtain *de novo* sequencing information for a few of the dominant IgG1 and IgA1 antibodies by a combination of bottom-up and top-down mass spectrometry approaches. When comparing these sequences with those deposited in the Cov-AbDab database, we found that especially the IgG1 clones had underlying germline sequences (IGxV + IGxJ genes) that were among the top 10 and top 20 for the light and heavy chains, respectively, when compared to the database of nearly 10,000 human antibody entries (20, 33). This advocates for the potential existence of a 'public' response at the level of clonotypes, despite the very clear individual response at the clonal level. For the here sequenced IgA1 clones, we did not observe an alike SARS-COV-2-specific gene usage. However, the Cov-AbDab database might not provide the same coverage for IgA and IgG isotypes, and sequencing of a higher number of IgA1 clones would be required to draw conclusions on the immunological role of this isotype in SARS-COV-2 infection. Furthermore, the sequences stored in the database are predominantly Spike-protein directed, whereas the IgA response has been shown to be stronger against the nucleocapsid protein than against Spike, particularly in the early phase (19, 34). Summarizing, although factors determining which antibody isotype is used against a certain pathogen may be unknown, when IgG1-based responses are triggered, our data support preferential gene usage.

This study and our previous studies have revealed a dominance of only a limited number of clones in serum IgG1 and IgA1 repertoires. To some, this raised the question whether what we see is not just the so-called "tip of the iceberg". In the current study, we therefore compared the Fab-based quantitation with our recent quantitative data-independent acquisition dataset of the same samples. We found a fairly high similarity in the quantities of IgG1 and IgA1 as determined by the two methods. These two complementary methods of quantitation also revealed that IgG1 and IgA1 concentrations in individuals may deviate substantially from the textbook-reported concentrations. Of note, the current study involves elderly donors, and increased age has been associated with lower antibody repertoire diversity (35). Whether the quantitation matches this well in donors of younger age is yet to be determined.

In addition to the biological hypothesis-generating findings described in this manuscript, we found proof of the value of our method for monoclonal antibody treatment pharmacokinetics. Without prior knowledge, we identified a common clone in multiple donors. This turned out to be tocilizumab, a therapeutic monoclonal antibody. Pharmacokinetics of human antibodies are difficult to study because of the high similarity with endogenous antibodies. Therefore, specific detection protocols need to be established for each compound, often including the generation of, for example, anti-idiotype antibodies (36). Using the approach presented here, any IgG1 monoclonal antibody—or even combinations thereof—can be detected and quantified over time to determine the relation between dose and serum concentration, as well as *in vivo* half-life like we showed here for tocilizumab. Furthermore, the technology could be used to support therapeutic drug monitoring-guided clinical decision making (37), especially in combination with size-exclusion chromatography, as demonstrated in our previous work (38). This aids to focus on functionally active mAbs (*e.g.*, not in complex with antigen or antidrug antibodies), a feature not often possible with other techniques (36). Although not available in every hospital, the potential cost reduction due to highly personalized therapeutic antibody monitoring may make it beneficial to perform the analysis at sites where it is available.

To conclude, we show that donors' responses against a common pathogen are highly personalized. Also, we provide evidence for the functional application of our methodology in a pharmaceutical or clinical setting for the monitoring of monoclonal antibody therapeutics. The case presented here advocates that clinical diagnostic tools need to be further advanced and become more personalized, as each person has its own response to pathogens and diseases, but also react differently to treatments. We suggest that monitoring antibody repertoires in patients may be one of the more useful clinical tools to monitor serological immune responses in patients due to illness, medical treatment, or treatment resistance.

DATA AVAILABILITY

The raw spectra have been deposited in the MassIVE repository with identifier MSV000091179.

Supplemental data—This article contains supplemental data.

Acknowledgments—We kindly acknowledge the teams of Janine Schuurman and Frank Beurskens, Boris Bleijlevens (Genmab) for continuous support over the years, stimulating discussions, financial co-support for A. B. and S. T., and the kind donation of IgG1-Campath and IgA1-7D8. We thank Dietmar Reusch and Markus Haberger (Roche) for the kind donation of trastuzumab.

Funding and additional information—The research was supported by Dutch Research Council (NWO) funding the Netherlands Proteomics Centre through the X-omics Road Map program (project 184.034.019) and the EU Horizon 2020 program INFRAIA project Epic-XS (Project 823839) and by the Dutch Research Council NWO Gravitation 2013 BOO, Institute for Chemical Immunology (ICI; 024.002.009) and the Utrecht Molecular Immunology Hub.

Author contributions—A. B., S. S., P. R., and A. J. R. H. conceptualization; A. B., S. S., P. R., and A. J. R. H. methodology. A. B., M. H., K. D., S. T., W. P., M. A. de B., M. D., C. Z., Arjan Barendregt, D. M. H. van R., M. G., K. T., J. van R., and F. V. investigation. A. B., M. H., S. T., B. de G., W. P., M. G., J. S., and M. J. van G. formal analysis. F. F., A. P., C. A. V., G. C., M. C., S. S., and P. R. resources. A. B., M. H., S. T., W. P., and A. J. R. H. writing-original draft; A. B., B. de G., J. S., M. J. van G., M. H., K. D., S. T., W. P., M. A. de B., M. D., C. Z., D. M. H. van R., M. G., K. T., J. van R., S. S., Arjan Barendregt, P. R., A. J. R. H., F. F., A. P., C. A. V., G. C., M. C., and F. V. writing-review and editing.

Conflict of interest—The authors declare no competing interests.

Abbreviations—The abbreviations used are: ACN, acetonitrile; BMI, body mass index; CDR, complementarity determining region; Cov-AbDab, COVID antibody database; COVID-19, Corona virus disease 2019; ETD, electron transfer dissociation; FDA, Food and Drug Administration; ICU, intensive care unit; Ig, Immunoglobulin; Mw, molecular weight; RBC, red blood cells; RBD, receptor-binding domain; RT, retention time; RT-PCR, real-time polymerase chain reaction; SARS-CoV-2, severe acute respiratory syndrome corona virus 2.

Received September 27, 2023, and in revised form, November 30, 2023 Published, MCPRO Papers in Press, December 6, 2023, https://doi.org/10.1016/j.mcpro.2023.100690

REFERENCES

1. Schroeder, H. W., Jr. (2006) Similarity and divergence in the development and expression of the mouse and human antibody repertoires. *Dev. Comp. Immunol.* **30**, 119–135
2. Briney, B., Inderbitzin, A., Joyce, C., and Burton, D. R. (2019) Commonality despite exceptional diversity in the baseline human antibody repertoire. *Nature* **566**, 393–397
3. Bondt, A., Hoek, M., Tamara, S., de Graaf, B., Peng, W., Schulte, D., *et al*. (2021) Human plasma IgG1 repertoires are simple, unique, and dynamic. *Cell Syst.* **12**, 1131–1143.e1135
4. Bondt, A., Dingess, K. A., Hoek, M., van Rijswijck, D. M. H., and Heck, A. J. R. (2021) A direct MS-based approach to profile human milk secretory immunoglobulin A (IgA1) reveals donor-specific clonal repertoires with high longitudinal stability. *Front. Immunol.* **12**, 789748
5. Lee, J., Paparoditis, P., Horton, A. P., Fruhwirth, A., McDaniel, J. R., Jung, J., *et al*. (2019) Persistent antibody clonotypes dominate the serum response to influenza over multiple years and repeated vaccinations. *Cell Host Microbe* **25**, 367–376.e365
6. Wine, Y., Boutz, D. R., Lavinder, J. J., Miklos, A. E., Hughes, R. A., Hoi, K. H., *et al*. (2013) Molecular deconvolution of the monoclonal antibodies that comprise the polyclonal serum response. *Proc. Natl. Acad. Sci. U. S. A.* **110**, 2993–2998
7. Tu, C., Rudnick, P. A., Martinez, M. Y., Cheek, K. L., Stein, S. E., Slebos, R. J., *et al*. (2010) Depletion of abundant plasma proteins and limitations of plasma proteomics. *J. Proteome Res.* **9**, 4982–4991
8. Demichev, V., Tober-Lau, P., Nazarenko, T., Lemke, O., Kaur Aulakh, S., Whitwell, H. J., *et al*. (2022) A proteomic survival predictor for COVID-19 patients in intensive care. *PLOS Digit Health* **1**, e0000007
9. Vollmy, F., van den Toorn, H., Zenezini Chiozzi, R., Zucchetti, O., Papi, A., Volta, C. A., *et al*. (2021) A serum proteome signature to predict mortality in severe COVID-19 patients. *Life Sci. Alliance* **4**, e202101099
10. Geyer, P. E., Arend, F. M., Doll, S., Louiset, M. L., Virreira Winter, S., Muller-Reif, J. B., *et al*. (2021) High-resolution serum proteome trajectories in COVID-19 reveal patient-specific seroconversion. *EMBO Mol. Med.* **13**, e14167
11. Demichev, V., Tober-Lau, P., Lemke, O., Nazarenko, T., Thibeault, C., Whitwell, H., *et al*. (2021) A time-resolved proteomic and prognostic map of COVID-19. *Cell Syst.* **12**, 780–794.e787
12. Campo, G., Contoli, M., Fogagnolo, A., Vieceli Dalla Sega, F., Zucchetti, O., Ronzoni, L., *et al*. (2021) Over time relationship between platelet reactivity, myocardial injury and mortality in patients with SARS-CoV-2-associated respiratory failure. *Platelets* **32**, 560–567
13. Vieceli Dalla Sega, F., Fortini, F., Spadaro, S., Ronzoni, L., Zucchetti, O., Manfrini, M., *et al*. (2021) Time course of endothelial dysfunction markers and mortality in COVID-19 patients: a pilot study. *Clin. Transl. Med.* **11**, e283
14. Spadaro, S., Fogagnolo, A., Campo, G., Zucchetti, O., Verri, M., Ottaviani, I., *et al*. (2021) Markers of endothelial and epithelial pulmonary injury in mechanically ventilated COVID-19 ICU patients. *Crit. Care* **25**, 74
15. Contoli, M., Papi, A., Tomassetti, L., Rizzo, P., Vieceli Dalla Sega, F., Fortini, F., *et al*. (2021) Blood Interferon-α levels and severity, outcomes, and inflammatory profiles in hospitalized COVID-19 patients. *Front. Immunol.* **12**, 648004
16. Grobben, M., van der Straten, K., Brouwer, P. J., Brinkkemper, M., Maisonnasse, P., Dereuddre-Bosquet, N., *et al*. (2021) Cross-reactive antibodies after SARS-CoV-2 infection and vaccination. *Elife* **10**, e70330
17. Schulte, D., Peng, W., and Snijder, J. (2022) Template-based assembly of proteomic short reads for de novo antibody sequencing and repertoire profiling. *Anal. Chem.* **94**, 10391–10399
18. van Rijswijck, D. M. H., Bondt, A., Hoek, M., van der Straten, K., Caniels, T. G., Poniman, M., *et al*. (2022) Discriminating cross-reactivity in polyclonal IgG1 responses against SARS-CoV-2 variants of concern. *Nat. Commun.* **13**, 6103
19. Sterlin, D., Mathian, A., Miyara, M., Mohr, A., Anna, F., Claër, L., *et al*. (2021) IgA dominates the early neutralizing antibody response to SARS-CoV-2. *Sci. Transl. Med.* **13**, eabd2223
20. Raybould, M. I. J., Kovaltsuk, A., Marks, C., and Deane, C. M. (2021) CoV-AbDab: the coronavirus antibody database. *Bioinformatics* **37**, 734–735
21. Wang, D., Fu, B., Peng, Z., Yang, D., Han, M., Li, M., *et al*. (2021) Tocilizumab in patients with moderate or severe COVID-19: a randomized, controlled, open-label, multicenter trial. *Front. Med.* **15**, 486–494
22. Lemmens, H. J., Bernstein, D. P., and Brodsky, J. B. (2006) Estimating blood volume in obese and morbidly obese patients. *Obes. Surg.* **16**, 773–776
23. Nishimoto, N., Yoshizaki, K., Maeda, K., Kuritani, T., Deguchi, H., Sato, B., *et al*. (2003) Toxicity, pharmacokinetics, and dose-finding study of repetitive treatment with the humanized anti-interleukin 6 receptor antibody MRA in rheumatoid arthritis. Phase I/II clinical study. *J. Rheumatol.* **30**, 1426–1435
24. Williams, L. D., Ofek, G., Schatzle, S., McDaniel, J. R., Lu, X., Nicely, N. I., *et al*. (2017) Potent and broad HIV-neutralizing antibodies in memory B cells and plasma. *Sci. Immunol.* **2**, eaal2200
25. Peng, W., Pronker, M. F., and Snijder, J. (2021) Mass spectrometry-based de novo sequencing of monoclonal antibodies using multiple proteases and a dual fragmentation scheme. *J. Proteome Res.* **20**, 3559–3566
26. Guthals, A., Gan, Y., Murray, L., Chen, Y., Stinson, J., Nakamura, G., *et al*. (2017) De novo MS/MS sequencing of native human antibodies. *J. Proteome Res.* **16**, 45–54
27. Tran, N. H., Rahman, M. Z., He, L., Xin, L., Shan, B., and Li, M. (2016) Complete de novo assembly of monoclonal antibody sequences. *Sci. Rep.* **6**, 31730

28. Sen, K. I., Tang, W. H., Nayak, S., Kil, Y. J., Bern, M., Ozoglu, B., *et al*. (2017) Automated antibody de novo sequencing and its utility in biopharmaceutical discovery. *J. Am. Soc. Mass Spectrom.* **28**, 803–810
29. de Graaf, S. C., Hoek, M., Tamara, S., and Heck, A. J. R. (2022) A perspective toward mass spectrometry-based de novo sequencing of endogenous antibodies. *MAbs* **14**, 2079449
30. den Boer, M. A., Greisch, J. F., Tamara, S., Bondt, A., and Heck, A. J. R. (2020) Selectivity over coverage in de novo sequencing of IgGs. *Chem. Sci.* **11**, 11886–11896
31. Shaw, J. B., Liu, W., Vasil Ev, Y. V., Bracken, C. C., Malhan, N., Guthals, A., *et al*. (2020) Direct determination of antibody chain pairing by top-down and middle-down mass spectrometry using electron capture dissociation and Ultraviolet Photodissociation. *Anal. Chem.* **92**, 766–773
32. Mao, Y., Valeja, S. G., Rouse, J. C., Hendrickson, C. L., and Marshall, A. G. (2013) Top-down structural analysis of an intact monoclonal antibody by electron capture dissociation-Fourier transform ion cyclotron resonance-mass spectrometry. *Anal. Chem.* **85**, 4239–4246
33. Han, X., Wang, Y., Li, S., Hu, C., Li, T., Gu, C., *et al*. (2021) A rapid and efficient screening system for neutralizing antibodies and its application for SARS-CoV-2. *Front. Immunol.* **12**, 653189
34. Kurano, M., Morita, Y., Nakano, Y., Yokoyama, R., Shimura, T., Qian, C., *et al*. (2022) Response kinetics of different classes of antibodies to SARS-CoV2 infection in the Japanese population: the IgA and IgG titers increased earlier than the IgM titers. *Int. Immunopharmacol.* **103**, 108491
35. Tabibian-Keissar, H., Hazanov, L., Schiby, G., Rosenthal, N., Rakovsky, A., Michaeli, M., *et al*. (2016) Aging affects B-cell antigen receptor repertoire diversity in primary and secondary lymphoid tissues. *Eur. J. Immunol.* **46**, 480–492
36. Ovacik, M., and Lin, K. (2018) Tutorial on monoclonal antibody pharmacokinetics and its considerations in early development. *Clin. Transl. Sci.* **11**, 540–552
37. Oude Munnink, T. H., Henstra, M. J., Segerink, L. I., Movig, K. L., and Brummelhuis-Visser, P. (2016) Therapeutic drug monitoring of monoclonal antibodies in inflammatory and malignant disease: translating TNF-α experience to oncology. *Clin. Pharmacol. Ther.* **99**, 419–431
38. Dingess, K. A., Hoek, M., van Rijswijk, D. M. H., Tamara, S., den Boer, M. A., Veth, T., *et al*. (2023) Identification of common and distinct origins of human serum and breastmilk IgA1 by mass spectrometry-based clonal profiling. *Cell. Mol. Immunol.* **20**, 26–37